Review

Ultramicroelectrodes: Design, Fabrication, and Characterization

*Cynthia G. Zoski**

Georgia State University, Chemistry Department, University Plaza, Atlanta, GA 30303, USA; e-mail: checgz@panther.gsu.edu

Received: January 18, 2002
Final Version: March 12, 2002

Abstract
Ultramicroelectrodes (UMEs) have led to unprecedented advances in electrochemical studies since their introduction to electroanalytical chemistry about twenty five years ago. During this time, several UME geometries have been reported of which disk, ring, ring-disk, hemispherical, spherical, and etched (finite cone) UMEs are the most commonly used. In this review, the design and fabrication procedures for each are described. Issues related to UME electrode surface treatment and characterization are also addressed.

Keywords: Ultramicroelectrodes, Nanoelectrodes, Nanodes, Disk electrode, Ring electrode, Ring-disk electrode, Hemispherical electrode, Conical Electrode, Etched electrode, Ultramicroelectrode fabrication

1. Introduction

Since their introduction to electroanalytical chemistry about 25 years ago, ultramicroelectrodes (UMEs) have led to unprecedented advances in electrochemical science. Though routinely used by physiologists [1] many years before electrochemists realized their advantages, the introduction of UMEs to electroanalytical chemistry occurred principally through the independent work of Wightman [2] and Fleischmann [3, 4] and their co-workers about 1980. Since that time, these devices have extended electrochemical methodology into broad new domains of space (single cells, membrane pores), time (steady-state, fast-sweep), chemical medium (nonaqueous solvents, unsupported electrolytes, ice, air), and methodology (kinetics, single molecule studies, AFM, STM, SECM) that are described in the many reviews that have been dedicated to their use [2 – 18].

UMEs, as the name implies, are smaller than "normal" electrodes, which generally have dimensions of meters, centimeters, or millimeters, depending on the application. The question of how small the dimension of an electrode has to be before it is considered a UME has been discussed but not resolved [8, 14]. However, it is generally accepted that a UME is an electrode which is smaller than the scale of the diffusion layer in readily achievable experiments. Thus, operationally, a UME has been defined as an electrode having at least one dimension, called the critical dimension, smaller than 25 μm [19]. This critical dimension could be the radius of a disk electrode or the width of a band or ring electrode. When the electrode's critical dimension becomes comparable to the thickness of the double layer or to the size of molecules, the experimental behavior of the electrode appears to deviate from theoretical expectations based on larger electrodes. Such behavior has been found to occur with electrodes of critical dimension smaller than about 10 nm [8, 20, 21] which can be considered the lower limit of a UME. Electrodes with critical dimensions smaller than 10 nm have been referred to as nanodes [22].

The versatility of UMEs arises due to their unique behavior, which is largely controlled by the interplay of current ($i\alpha a$), uncompensated resistance ($R_u\alpha 1/a$), and double layer capacitance ($C_d\alpha a$),where a is the radius of a disk UME. This includes the ability to operate in both early transient (e.g., Cottrellian conditions, $i\alpha t^{-1/2}$) or steady-state ($i\alpha a$) regimes. Early transient experiments are possible because the cell time constant ($R_uC_d\alpha a$) and the iR drop ($iR_u\alpha a$) both decrease as the electrode radius becomes smaller. Steady-state experiments are possible due to the enhanced mass transport that arises as a result of the curvature of the electrode. In steady-state experiments, the iR drop is a constant, dependent on the solution conductivity [5, 8, 9, 19].

Presently, the most popular UME geometries are those which reach a voltammetric steady-state and are small in all of their dimensions. Such geometries include inlaid disks, inlaid rings, inlaid ring-disks, shrouded hemispherical and spherical electrodes, and finite conical electrodes (or etched electrodes) (Fig. 1). This review considers the design, fabrication, and characterization of each of these geometries. Metal disk electrodes encapsulated in glass are considered first and in some detail, since these are easiest to fabricate. Although there are also many interesting applications of arrays [23, 24] of UMEs, potentiometric UMEs [25], and enzymatic UMEs [26] in electroanalysis, the literature on these geometries is too vast to consider in this review. Additionally, cylindrical and microband (line) electrodes [3, 5, 8] enjoyed some popularity in the 1980's because they provided large currents for an electrode molecularly small in one dimension but long in the other compared to the same size disk electrode, for example. At the time, they were also easier to fabricate than an inlaid disk electrode. Currently, however, they are much less popular than the other UME geometries because they do not reach a steady state and are not useful in eliminating iR drops. For

  1040-0397/02/1508-1041 $ 17.50+.50/0

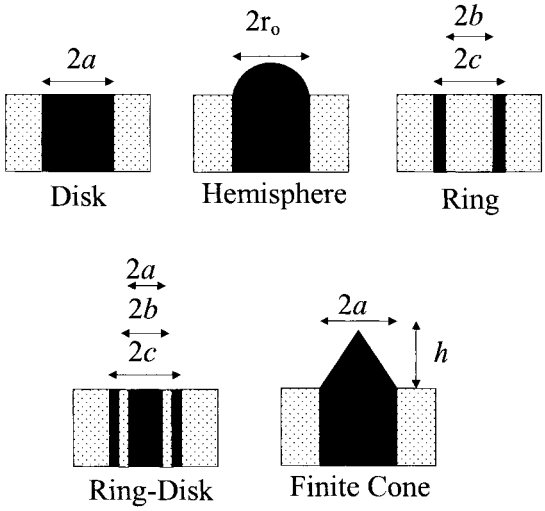

Fig. 1. Popular UME geometries. *a*: radius of disk or finite conical electrode; r_0: radius of hemispherical electrode; *b*: inner radius of ring electrode; *c*: outer radius of ring electrode.

these reasons, cylindrical and microband electrodes are also not considered in the present review.

2. Disk UMEs

2.1. Encapsulation in Glass

There are several excellent reviews with detailed accounts of sealing fine wires (≥ 10 μm diameter) of Pt, Au, or C into glass [3, 10, 27–29]. The following description is a combination of the reported procedures that the author has found to work in her laboratory. Basically, one begins with a length of wire (≈ 2 cm) which is inserted into a 10 cm long (2 mm outer diameter, 1 mm inner diameter) Pyrex glass (borosilicate) capillary. Soft or soda lime glass is used for Au wires. Before inserting the fine wire, the glass capillary is first sealed at one end using a bunsen burner or a minitorch. The open end of the tube is then connected to a vacuum line. One way to do this is to wrap the open end of the capillary with several layers of Teflon tape to form a gasket. This is inserted into the inlet of the vacuum source which can be made from a glass tube with an inner diameter that is slightly larger than the outer diameter of the capillary tube. When the capillary tube is placed in the larger glass tube and a vacuum applied, the Teflon gasket will form a good seal. This arrangement also serves to keep the capillary perfectly straight, when centered in a nichrome wire heating coil. The nichrome wire is usually between 18 and 22 gauge, and is coiled so that there are approximately 7 turns, with an inner diameter of approximately 5 mm and a length of approximately 1 cm. The nichrome coil can then be secured to a ceramic block which is mounted on a micromanipulator or alternatively mounted on a small laboratory jack. The purpose of either mount is to be able to move the coil up and down around the capillary tube, which is centered. The nichrome coil can be heated either with a DC power supply or with AC voltage from a Variac transformer. In either case, about 300 W of power is needed to melt the capillary. If a Variac is used (e.g., 120 V/10 A), then a step down transformer will be necessary for achieving the wattage needed for heating the 18–22 G nichrome coil to a temperature sufficient for melting Pyrex glass. The input of the transformer is connected to the Variac, and the output of the Variac controlled.

To begin the sealing process, the nichrome coil is moved so that the capillary is centered in the middle of the coil. The coil is preheated to a temperature just below a visible dull red color. This low temperature heating process is performed between 5 and 30 minutes; the purpose is to desorb any impurities or moisture on the wire and glass tube. The coil is then moved to the bottom of the capillary, the heat increased until the nichrome wire is a bright reddish-orange color, and the coil moved in 1 mm increments up the capillary as melting occurs at each increment. The glass should melt around the wire for at least 2–5 mm at the tip of the assembly. The entire capillary, including the part that seals the wire, should be straight; if it is bent or scorched at the tip, then the coil temperature is too hot. The heating coil is turned off, and the electrode allowed to cool. The electrode is then inspected under an optical microscope to make sure that there are no trapped air bubbles around the wire. The sealed end is polished with successive grades of coarse sandpaper (400, 600, 800, 1200 grit) to expose the wire, followed by successive grades of alumina (1, 0.3, 0.05 μm) until a scratch free surface is obtained under optical microscope examination. Electrical connection to the unsealed end of the wire is made by injecting silver epoxy into the capillary with a syringe and inserting a 30 gauge Cu wire wrap connecting wire. After curing the silver epoxy, the electrode can be finished by sealing the open end with quick drying epoxy. Additional steps can be taken to decrease stray capacitance effects if the UMEs are to be used in fast-scan cyclic voltammetry [30]. The grinding and polishing steps can be achieved by using a commercial polishing wheel or alternatively, a converted hard drive.

Fabrication of disk-shaped platinum electrodes of 1 to 5 μm diameter is similar to that described above but employs Wollaston wire. This is Pt wire with a 50–100 μm silver coating, which must first be removed with nitric acid. The procedure for working with these wires is consistently described in the literature [10, 27, 28].

In scanning probe techniques such as scanning electrochemical microscopy (SECM) [27, 28, 31], one is interested in bringing a UME into close proximity of a surface (the substrate) containing a system of interest, such as a cell or a piece of material that is undergoing a chemical change, in order to examine the chemistry on the surface with very high resolution. For a very close approach, an electrode on the order of 10 μm radius or smaller is required. Additionally, a very small glass shielding, the so-called RG ratio, is required. RG refers to the ratio of the radius of the glass shielding to the metal or carbon electrode radius. Normally, one strives to achieve an RG ≤ 10. A small RG decreases the

possibility of contact between glass shielding and substrate because of any slight deviation in the axial alignment of the tip as it approaches the substrate. The process is referred to as "sharpening" the electrode and is accomplished with 600, 1000, and 1200 grit SiC paper. One begins the sharpening by mounting the 600 grit SiC paper on a polishing wheel and grinding the end of the electrode, while rotating, at a 45° angle. The purpose of rotating the electrode is to make the glass shield as circular as possible. During this and subsequent grinding steps, one is frequently checking the status of the glass shielding dimension under an optical microscope. When the glass shield is reduced to about 300 μm in diameter compared to the metal electrode, 1000 grit SiC paper is used until the glass shield is reduced to about 100 μm compared to the metal electrode. The final step is done manually with "used" 1000 grit SiC or new 1200 grit SiC paper. With practice, one can reproducibly make electrodes with $RG \leq 10$.

2.2. Pulled Pt Wires/Pipette Puller

An alternative procedure for fabricating disk-shaped UMEs less than 2 μm diameter involves inserting metal wires into an open glass capillary and then pulling the metal/glass assembly together using a pipette puller [32 – 36]. Due to the fast and reproducible local heating of a glass capillary together with an inserted metal wire, the metal wire is pulled simultaneously with the glass leading to a drastic decrease of its diameter and a simultaneous tight seal of the metal within the glass capillary. In the earliest studies, 50 μm diameter annealed Pt wire was inserted into Pyrex capillaries and the metal/glass assembly pulled together. One programs the pipette puller with parameters that control the final shape and size of the glass capillary after the pulling step. These parameters include the temperature of heating of the glass and the strength of the pulling. After pulling, the metal core of the electrode is covered in glass and must be exposed. This can be done either by etching the glass with hydrofluoric acid or by micropolishing with a micropipette beveler fitted with a micromanipulator and long working distance stereomicroscope. In either method, the size of the final metal core increases with the length of time used to perform the etching or polishing. Under optimum conditions, UMEs with radii as small as 2 nm have been reported, though the shape of the metal core exposed by etching and micropolishing is significantly different. Etched electrodes usually have a finite conical shape, while micropolished electrodes generally have the geometry of an inlaid disk.

The exact fabrication procedure for using a laser pipette puller in fabricating UMEs down to 10 nm was recently reported [36]. In this study, quartz capillaries (half the thickness of capillaries generally used to make UMEs) and 25 μm hard Pt wire were used. A unique polishing procedure was also reported.

Pipette pullers have also been used in the fabrication of disk-shaped electrodes based on carbon fibers (5 – 40 μm diameter). A carbon fiber is first aspirated under low pressure into a glass capillary containing an inner filament. The capillary/carbon fiber assembly is then pulled in a pipette puller so that the glass is tapered around the fiber. The tip is then cut with a scalpel to expose the carbon fiber, placed in epoxy to obtain a seal between the glass and the fiber, and heat cured. A smooth surface is achieved by polishing with successively finer grades of alumina or diamond polish. Carbon fiber tips have also been beveled for use in neuronal cell studies [10, 11, 13, 37 – 40]. Using a similar procedure, a 7 μm diameter carbon fiber was inserted into a commercial Teflon capillary, followed by pulling the capillary to produce a self-sealing thin Teflon coating. The carbon fiber was exposed by cutting with a microsurgical scalpel blade. Due to the hardness of Teflon, cutting is the only means by which the carbon electrode surface can be renewed in these Teflon-coated UMEs [35].

Carbon disk UMEs have also been fabricated with tip diameters approaching 100 nm. Quartz capillaries are initially pulled down to a small tip (< 2 μm) by a micropipette puller. In one procedure, methane gas is forced through the pulled capillary while it is being pyrolyzed. By prolonging the pyrolysis time, a carbon deposit forms at the tip of the capillary thus producing a carbon disk electrode. Electrical contact is then made between the carbon deposit and a wire via a small mercury pool inside the capillary [41]. More recently, using a similar procedure and setup, a carbon disk geometry was obtained by pyrolyzing acetylene in a nitrogen atmosphere [42].

2.3. Gold Microbead UMES

Gold microbeads [43] of 1.5 to 3.0 μm diameter have been used to construct inexpensive and disposable microelectrodes with electrode diameters ≤ 5 μm. A micropipette puller was used to pull Pyrex capillaries (having an internal glass filament) to a tip opening of 2 μm. Because the pipette puller uses a preprogrammed series of heating, pulling, and stretching steps, pulled capillaries that are very uniform in shape and opening dimension can be produced. The presence of the glass filament in the capillary aids in filling the pulled capillary with gold beads that are injected as a suspension into the nontapered end of the pulled capillary. The water in the capillary is evaporated by placing the electrode assembly into an oven heated at 120 °C for an hour. Increasing the oven temperature to 580 °C for 2 hours, allows the gold beads to sinter into a solid mass. Epoxy is used to provide a leak-proof seal of the gold beads in glass. Electrical contact between the gold beads and external circuits is made with an electrolyte filling solution.

A reported advantage of the use of microscopic metal particles to make UMEs compared to microwires is that they are inexpensive and particles are available in smaller dimensions than metal microwires. Additionally, metal particles are reported to be easier to handle as suspensions in water, thus avoiding the fragility of microwires.

2.4. Chemical Vapor Deposition Fabrication

Carbon fiber and metal disk UMEs have also been fabricated by chemical vapor deposition (CVD) techniques [44–46] to insulate the cylindrical length of a C fiber or metal wire with a thin film of silica. Film formation occurs by deposition of silica from a $SiCl_4$, H_2, and O_2 gas phase precursor or by sequential deposition from $Si(OEt)_4$ (Silicon tetraethoxide) as a single source precursor followed by the $SiCl_4$, H_2, and O_2 precursor system. The latter protocol has been found to improve the adhesion of the silica film to the C fiber or metal wire, while $SiCl_4$ is the better precursor for obtaining thicker and stronger silica films. The silica deposition occurs directly on a resistively heated C fiber or metal wire. There is a temperature gradient near the fiber or metal end which results in variable deposition rates, and consequently, a uniform and concentric silica film which gradually tapers down to the bare C fiber or metal substrate. A diamond fiber optics cleaver is then used to produce a clean tip surface. Thus transparent silica films with a thickness up to 600 μm are deposited, but by choosing where the coated C fiber or metal wire is cut, the silica film at the tip can be less than 1 μm. Since the silica film is optically transparent, the C fiber or metal wire can be seen and used as an approximate scale for the diamond cut. The tip end is then polished using successive grades of alumina or diamond polish. Carbon fiber disk UMEs of 5 and 10 μm diameter have been fabricated in this way, with silica films ranging from 1 to 600 μm in thickness [44, 45].

In fabricating metal-based disk UMEs, initially a 25 μm diameter tungsten wire is concentrically coated with an insulating layer of silica. Some of the tungsten metal is then removed by electrochemical etching in hydroxide solution leaving a well-defined microcavity at the electrode tip. This silica-coated tungsten UME platform can then be used to make novel disk UMEs by incorporating materials with a high degree of selectivity towards a particular analyte. For example, copper and silver were electrodeposited into the microcavity from aqueous solutions of the respective cations. The resulting copper disk UME was used for the detection of glucose, while the silver disk UME was used to monitor chloride ions [46].

There are several reported advantages of this chemical vapor deposition-resistive heating (CVD-RH) technique [44–46]. First, electrode materials of various shapes and sizes can be modified with a wide range of coatings and thickness by changing the precursor system and deposition parameters. Film growth occurs directly at the heated electrode surface, so that excellent adhesion is obtained alleviating the need for sealants. The concentric deposition around the electrode translates into well-defined electrode geometries that conform to theoretical predictions.

3. Hemispherical and Spherical UMEs

3.1. Hemispherical UMEs

Hemispherical UMEs are generally fabricated using mercury [47–50]. Most often mercury ions are reduced at the surface of a disk-shaped metallic or carbon UME according to the reaction:

$$Hg_2^{2+}(aq) + 2e \rightarrow 2Hg(l) \quad (1)$$

Because mercury should wet the substrate surface but not form an amalgam with it, the substrate choice for mercury deposition is critical. Iridium has been found to be the most suitable substrate material, while platinum and carbon are relatively acceptable but worse substrates for mercury deposition. The growth of mercury on the chosen substrate is monitored by recording the time variation in the reduction current of the mercury ion. From the amount of mercury deposited, assuming hemispherical growth, the radius of the UME can be calculated. Optical microscopy has also been used to observe the hemispherical growth of Hg on a substrate. The radii of these UMEs appear to be equal to or larger than that of the supporting disk-shaped electrode.

3.2. Spherical UMEs

Spherical UMEs have been fabricated with diameters of 1 to 30 μm by self-assembly of gold nanoparticles and 1,9-nonanedithiol molecules at the tip of glass capillaries that have been pulled in a laser micropipette puller [51]. This technique was based on earlier work involving nanometer-sized Au particles where it was found that such particles could be self-assembled to electronically conductive bulk materials [52] and multilayer thin films [53] by use of dithiol cross-linking agents. To prepare the spherical UMEs, the dithiol linking agent was confined to the tip lumen of a pulled capillary, the inside of which had first been coated with a conductive carbon coating. This assembly was then immersed in a solution of Au particles, forcing the encounter of the Au particles and of the dithiol linker to occur only at the very end of the tip. A smooth spherical shiny sphere was observed to form at the end of the tip. This spherical geometry which resulted was found to be perfectly controlled and reproducible. The electrodes were found to have the electrochemical properties of metallic Au and showed ideal microelectrode behavior both in aqueous and in acetonitrile electrolyte solutions.

4. Inlaid Ring UMEs

The first ring electrodes were fabricated by applying a conductor to the walls of an insulating cylindrical support [54–57]. Most often the insulating support was a glass rod or, for smaller diameter rings, a flame-drawn glass rod. For

metal rings, the insulating support was either painted with organometallic compounds, or coated by vapor deposition or sputtering of metal onto a rotating glass rod. The vapor deposition method ensured a more uniform coating of the metal and permitted rings of thickness ranging from 10 nm to 5 μm to be fabricated. Both Pt and Au rings have been prepared by either method. The coated support was then insulated from solution by sealing into a larger glass tube with epoxy resin or by collapsing the glass around the rod. The structure was then sectioned and polished to expose the inlaid ring.

Carbon ring electrodes have been fabricated by depositing carbon on the inner surface of a pulled quartz capllary tube by pyrolyzing methane as it passes through the capillary. Once a shiny black carbon ring is produced, the tip is filled with epoxy, cured, and then trimmed or beveled to expose a fresh electroactive carbon surface [57 – 58].

In the past ten years, ring-shaped electrodes have been of special interest in connection with optical fiber probes for use in photoelectrochemical experiments [59 – 61] and photoelectrochemical microscopy (PEM) [62 – 64]. In these studies, the ring electrode was fabricated, in part, by using commercially available gold-coated optical fibers, by depositing a gold layer onto the shaft of an optical fiber, or by etching an optical fiber followed by gold deposition. The probes were then electrically insulated by dip coating in an insulating polymer or epoxy gluing the coated fiber into larger glass pipette tips. The result is a probe which can serve not only as a light source at the tip but also as a UME with an inner core diameter ranging from 2 – 400 μm and a ring thickness ranging from 2 – 35 μm.

More recently there has been interest in combining scanning electrochemical microscopy (SECM) [31] and near field scanning optical microscopy (NSOM) [65 – 68] in a technique referred to as scanning electrochemical/optical microscopy (SECM/OM) [69]. The fabrication of SECM/OM probes [69, 70] follows a procedure based on that used in the fabrication of NSOM tips [68, 71 – 74] which includes heating and pulling optical fibers in a laser-based pipette puller, metal coating of only the optical fiber shaft, electrical insulation, and exposing the ring electrode at the end of the tips. To fabricate SECM/OM probes, the pulled optical fiber was coated with Au by vacuum evaporation, followed by simple insulation of the tip end by electrodeposition of electrophoretic paint. Durable SECM/OM UMEs having the geometry of a ring with < 1 μm as the outer ring radius are reported. An "electro-optical" sensor [18] has also been reported which is based on a fabrication method similar to that described for the SECM/OM probes, except that the insulation is achieved by epoxy gluing a gold-coated pulled fiber into a pulled glass capillary. Only one electro-optical probe was reported, and this probe had an outer ring radius of 2 μm, which is larger than the fabricated SECM/OM probes.

5. Ring-Disk UMEs

There have been two separate reports regarding the fabrication of ring-disk UMEs. The first is based on the C disk UME, described in Section 2.4., in which a 10 μm diameter C fiber is insulated with a silica film by a CVD-RH technique. When the desired thickness of silica is deposited, the CVD reactor is purged with Ar and a layer of pyrolytic C is deposited from acetone. The silica coating process is repeated to insulate the newly-deposited C ring layer. The ring-disk UME is then prepared by cutting the end of the coated fiber at a position that produces the desired outside diameter for the analytical tip and polished. Tip diameters as small as 25 – 30 μm were fabricated [75].

A Au/Pt ring-disk UME has more recently been fabricated using a glass encapsulated Pt disk UME (10 and 25 μm diameter Pt wire) as described in Section 2.1. The UME tip was then sharpened until the desired RG factor was reached. A thin Au film was then sputtered onto the continuously rotated tip producing a thin Au film of about 500 nm. Insulation of the ring layer was achieved by coating with a commercial nail polish which was applied to the tip with a small brush by hand and allowed to dry in air at room temperature. The ring-disk assembly was exposed by polishing with aluminum oxide grinding paper [76].

6. Finite Conical (Etched) UMEs

Electrochemical etching of metal wires in order to fabricate electrodes in the range of ten nanometers to several micrometers has been used since 1978 [22, 29, 77 – 85]. The electrochemical etching procedure usually involves anodic dissolution of a metal as a result of applying an AC voltage. Several etching solution baths have been used. For etching Pt, Ir or Pt-Ir microwires, etching baths have been composed of saturated $CaCl_2$, H_2O, and concentrated HCl [29, 80, 81, 84], or concentrated $NaNO_2$ [82, 83], or NaCN and NaOH [78, 79] . For etching Au and Ag microwires, the etching solution is composed of NaCN and NaOH, while saturated NaOH solution is used for W wire etching [29]. The alternating voltage is applied between the microwire and a Pt coil in which the microwire is centrally located to ensure symmetrical etching of the microwire. There are tricks involved in getting a very sharp tip that depend on the etching current (which is a function of the area of immersed microwire and the applied voltage) and the length of time that the etching is allowed to proceed. Additionally, repeated etching in the same solution weakens the solution, so that it has been observed that the best tips are obtained with freshly made solutions. Etching solutions have also been found to become ineffective when stored for an extended period of time.

After etching, the tips are washed with copious amounts of triply distilled water to remove any residual etching solution. The etched ultrafine wires are then coated with an insulating material, except at the apex of the wire, thus providing a very tiny exposed electrode area. A number of

coating procedures have been employed, including RF sputtering [86] of insulating materials, or a simple dipping technique with a varnish [87, 88] or molten paraffin [89]. Translating the tip through a molten bead of glass [22, 79], poly(α-methylstyrene) [79], or apiezon wax [78, 80] held on a heated support, has also been adopted as a method for applying an insulating coating to the etched wire. Electrodes with submicrometer dimensions have also been prepared by electrodepositing insulating layers onto the metal surface [69, 70, 82 – 85, 90 – 95]. In particular, electrophoretic paints (anodic and cathodic) are commercially available and have been used to coat Pt-Ir STM tips [90 – 95], Pt SECM/AFM tips [85], Au SECM/OM tips [69, 70], and Pt UMEs [82, 83]. Anodic paint consists of poly(acrylic acid)(PAAH) with an excess of base added to make it water-soluble by deprotonation of the acidic groups thus forming the PAA^- species. The etched wire is immersed in a dilute aqueous paint solution and positioned in the center of a Pt coil. A DC potential is applied between the etched wire and the Pt coil. An anodic current flow produces a local pH decrease at the electrode surface, induced by water oxidation, and generates water insoluble PAAH that deposits onto the etched metal surface. During heat curing, the insulating layer shrinks so that the sharp end of the tip is exposed, while the shaft of the tip is completely insulated. Usually, a second insulation is carried out with more dilute anodic paint solution followed by the same curing to insure any pinholes formed in the first curing are sealed.

If electrophoretic paint is not used to insulate, then removal of the insulating material at the end of the tip to open up a metal electrode is usually attained by polishing or cutting [44, 45, 59, 61 – 64, 86, 94, 96], although milling with a focused electron [97] or ion beam [98] or touching the tip to a surface using scanning tunneling microscopy [80] have also been reported.

Carbon fibers have been etched to tip diameters in the range of 100 nm or smaller by passing the fiber slowly through an oxygen/methane flame, and then electrochemically coating with a thin poly(oxyphenylene) film for insulation [94]. Following a similar flame etching procedure, an etched carbon fiber has been sealed in glass, thus alleviating the need for an insulation step [99]. Carbon fibers have also been electrochemically etched in a NaOH bath to produce an active tip with an effective radius of 1 nm [100]. The electrochemically etched fiber is then insulated by the deposition of cathodic electrophoretic paint using an inverted deposition technique which is reported to lead to complete insulation of the entire shaft of the etched carbon fiber except for the very tip [100].

7. Microfabricated UMEs

Microfabrication technology has been used in UME fabrication in an attempt to enable reproducible construction of very small tips having an exact geometry [98, 101, 102]. Finite conical UMEs have been microfabricated through the anisotropic etching of silicon, followed by thin-film deposition of silicon dioxide, platinum and silicon nitride. Photoresist was applied so that the top of the tips were left just emerging from the photoresist layer. The silicon nitride layer was then removed from the tip region only by plasma etching, leaving a Pt finite cone having a base of radius of 1.25 μm and a height of 2 μm [102].

Pt disk-shaped UMEs have been microfabricated using through-mask plating on wafers having the structure Si(substrate)/SiO_2/Pt(plating base). A blanket SiO_2 mask layer was deposited by plasma-enhanced chemical vapor deposition and patterned using an organic photoresist mask so that an empty well was left between two SiO_2 mask towers. The photoresist was removed, Pt was plated into the well, followed by removal of the SiO_2 mask and Pt plating base. A Pt disk remained with dimensions including a 0.18 μm diameter and 0.2 μm height above the Si/SiO_2 wafer [103] surface.

Another microfabrication procedure begins with a standard AFM cantilever which is sputter coated with Au, insulated with silicon nitride, and then milled using a focused ion beam (FIB). The result is a boxed shaped electrode called a frame UME with an inner edge of 0.6 μm and outer edge of 0.75 μm [98].

8. UME Electrode Surface Treatment

Conventional methods of cleaning electrode surfaces to obtain consistent electrochemical responses usually include physical polishing of the electrode surface with either alumina particles or diamond paste. Polishing UMEs having a total structural diameter below about 1 μm has proven to be difficult, however, often resulting in broken electrode tips. Especially in the case of submicrometer electrodes, it appears that electrodes are replaced, rather than rejuvenated, once they begin showing uncharacteristic behavior. At this time, there appears to be no simple solution to this dilemma.

Pulse techniques [104 – 108] have been used to obtain predictable and renewable electrode surfaces without polishing. One method, pulsed amperometric detection (PAD) has been used frequently. In this method, a large anodic pulse results in the desorption of surface-bound species, and causes a thin layer of oxide to be formed at the electrode surface. A second cathodic pulse causes the dissolution of the oxide film and reactivates the electrode surface. The potential is then changed to a value at which the detection occurs.

Pt electrodes can be cleaned and "activated" by cycling in 1 M H_2SO_4 between potentials where hydrogen evolution occurs and potentials where oxygen evolution occurs. The cycling should end with the cathodic phase. After several cycles, the voltammogram of the Pt electrode should show peaks for the formation and oxidation of both adsorbed hydrogen and adsorbed oxygen [109].

There is a wealth of information available on the treatment of carbon UMEs [110, 111]. Very recent reports have looked at the effects of potentiodynamic and potentiostatic

activation of glassy carbon surfaces [112] and the UV/ozone pretreatment of glassy carbon electrodes [113].

Recently, a polishing device, based on a rotating disk electrode configuration, has been described for polishing newly pulled UMEs or for repolishing already used ones. Polishing is achieved by rotation (5000 rpm) of the UME and, with the aid of micropositioners, slowly lowering the UME tip onto a stationary polishing plate. Polishing paper or polishing cloth is adhered to the polishing plate, and polishing is performed in either a droplet of water or in alumina polishing paste. Pulled UMEs with radii below 10 nm have been polished in this way [36].

9. UME Characterization

Once fabricated, UMEs are generally characterized by scanning electron microscopy (SEM), steady-state voltammetry (SSV), and more recently by scanning electrochemical microscopy (SECM).

In SEM micrographs, one primarily looks for a good seal between the metal or fiber and insulating material at the tip end. Sometimes it is possible to obtain an estimate of the radius of the electrode as well as the radius of the insulating material. From side images, one looks to see whether the metal or fiber is in the plane of, recessed within, or protruding from the insulating material. Side-view images can also provide information regarding the integrity of the insulating medium (e.g., is the surface smooth and devoid of pinholes or cracks) [29, 34, 36, 69, 82, 84].

In characterization studies, steady-state voltammetry (SSV) can provide an estimate of the radius of the UME and demonstrate that the electrode response follows theory. When using SSV in this way, well-characterized systems having rapid heterogeneous electron transfer are used. Commonly used aqueous systems include the oxidation of ferrocene methanol (1 mM, 50 mM TMAP (tetramethyl ammonium perchlorate), $D = 7.8 \times 10^{-6}$ cm^2/s [114]),

$$FcCH_2OH \rightarrow FcCH_2OH^+ + e \quad (2)$$

the oxidation of ferrocyanide (1 mM, 0.1 M KCl, $D = 6.5 \times 10^{-6}$ cm^2/s [115]),

$$Fe(CN)_6^{4-} \rightarrow Fe(CN)_6^{3-} + e \quad (3)$$

the reduction of ruthenium hexamine (1 mM, 0.09 M Na_3PO_4, $D = 5.3 \times 10^{-6}$ cm^2/s [10]),

$$Ru(NH_3)_6^{3+} + e \rightarrow Ru(NH_3)_6^{2+} \quad (4)$$

and the reduction of ferricyanide (1 mM, 0.1 M KCl, $D = 7.6 \times 10^{-6}$ cm^2/s [115]),

$$Fe(CN)_6^{3-} + e \rightarrow Fe(CN)_6^{4-} \quad (5)$$

In SSV at UMEs, the potential is swept slowly and triangularly as shown in Figure 2. The resulting current-potential curve is sigmoidal in shape and retraces on the return sweep. A gap in the forward and backward branches is an indication that the sweep rate is too fast, or that there is a poor seal between the insulator and metal wire or carbon fiber. Features of the reversible steady-state wave are shown in Figure 3. These include a diffusion-limited plateau current (i_{dif}), a half-wave-height current ($i_{1/2}$) and potential ($E_{1/2}$), and the quartile currents ($i_{1/4}$, $i_{3/4}$) and potentials ($E_{1/4}$, $E_{3/4}$). The diffusion-limited plateau current depends on the geometry of the electrode and, for the UME geometries considered in this article, is defined as [9, 116]

$$i_{dif} = 2\pi nFDc^b r_0 \quad \text{hemisphere} \quad (6)$$

$$i_{dif} = 4nFDc^b a \quad \text{disk} \quad (7)$$

$$i_{dif} = nFDc^b l_0$$
$$l_0 = [\pi^2 (b + c)]/\ln [16(b + c)/(c - b)],\ c/b < 1.25 \quad \text{ring} \quad (8)$$

$$i_{dif} = 4nFDc^b a(1 + qH^P),\ q = 0.3661,\ p = 1.14466,$$
$$H = h/a \quad \text{finite cone} \quad (9)$$

where n is the number of electrons, F is the Faraday constant, D is the diffusion coefficient, c^b is the bulk concentration of

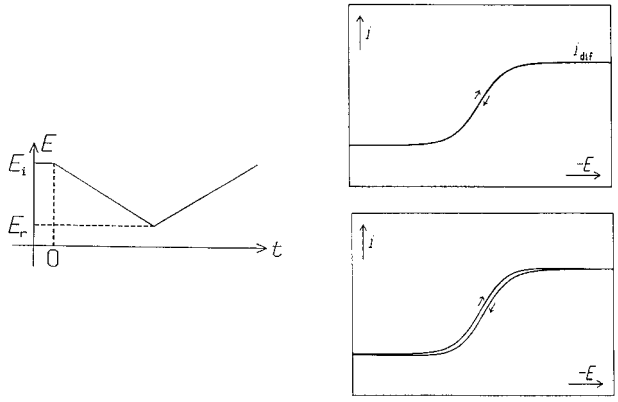

Fig. 2. Potential waveform and steady-state current-potential waves. E_i: initial potential; E_r: reversal potential; i_{dif}: diffusion-limited plateau current.

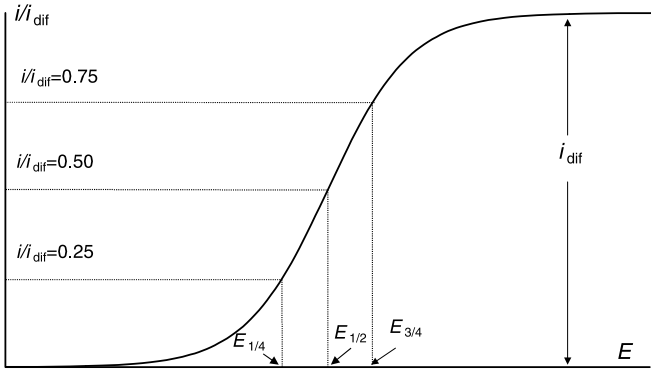

Fig. 3. Features of a steady-state voltammogram including half wave-height current ($i/i_{dif} = 0.50$) and potential ($E_{1/2}$), quartile currents ($i/i_{dif} = 0.25$, $i/i_{dif} = 0.75$) and potentials ($E_{1/4}$, $E_{3/4}$).

electroactive species, r_0 is the radius of the hemisphere, a is the radius of a disk or the basal radius of a finite cone, b is the inner ring radius, c is the outer ring radius, and h is the finite cone height (Fig. 1). Using these equations, the electrode radius for a specific UME geometry can be determined and compared to values obtained from optical microscopy and SEM micrographs. The shape of the steady-state wave can be determined from the quartile potentials according to the Tomes criterion ($|E_{3/4} - E_{1/4}| = 56.4/n$ mV) and a log plot analysis (E vs. log $[(i_{dif} - i)/i]$, slope = 59.1/ mV, intercept = $E_{1/2}$) for reversible systems.

It is important to note that if a UME is formed by etching a wire and then insulated by translating through a molten bead of glass [22, 79], poly(α-methylstyrene) [79], or apiezon wax [78, 80], then there is a good likelihood that the metal will be recessed within the insulating material. A diffusion-limited plateau current will be obtained that is smaller in magnitude than that given by Equations 6, 7, or 9. Thus, an electrode radius that is calculated using these equations, will be smaller than the true radius. The recessed UME can be detected using SECM, as described below.

In the past few years, scanning electrochemical microscopy (SECM) has been shown to be invaluable in evaluating the size and shape parameters of a UME. In SECM, a UME tip is brought in close proximity to an electrically insulating or conductive substrate [31, 34, 70, 80, 85]. Approach curves resembling those shown in Figure 4 for an inlaid disk UME are recorded and compared to theoretical curves. When the UME is far from a substrate, the diffusion-limited current, $i_{T,\infty}$, is measured due to either reduction or oxidization of a redox mediator at the tip surface. The subscript ∞ implies this long distance, whereas the subscript T is used to denote the UME as the tip electrode; thus $i_{T,\infty}$ is the same as i_{dif} defined in Equations 6–9. When the UME tip is brought within a few tip diameters of an infinitely large conducting substrate, like a platinum electrode, the product of the tip reaction diffuses to the substrate where it may be re-oxidized or re-reduced. This process produces an enhancement, or positive feedback, in the UME tip current ($i_T > i_{T,\infty}$) which depends on the tip shape and the tip-substrate separation d. For example, when an inlaid disk serves as the tip UME, its entire surface is facing the substrate such that its distance from the substrate is the same for every point on the UME tip surface. When the UME tip has the geometry of a finite cone, then the sharp point of the cone prevents an interaction between the main part of the UME tip and the substrate. This results in a positive feedback current approach curve which differs from that seen for an inlaid disk [34, 80]. A similar effect has been shown for hemispherical [50], ring [70], and ring-disk [76] UME tips. When the UME tip is brought within a few diameters of an infinitely large insulating substrate, like a piece of glass or plastic, then the substrate blocks some of the diffusion of the mediator to the UME tip, and the current decreases compared to $i_{T,\infty}$ ($i_T < i_{T,\infty}$) as shown as the lower curve in Figure 4. Since no reaction occurs at the insulating substrate, this decrease in current with distance is called negative feedback. It has been shown that the negative feedback current is relatively insensitive to the geometry of the UME tip, so that UME geometry determinations are usually performed in the positive feedback mode. Similarly, the insulator layer thickness (RG) has been shown to affect SECM approach curves for insulating substrates more obviously than for conductive substrates, so that RG determinations are generally carried out in the negative feedback mode [70, 80]. Thus the information that one is able to obtain from SECM approach curves includes the UME tip geometry and radius, and the RG value of the insulation.

SECM can also be used to check for complete electrical insulation on the sides of a UME by recording approach curves at an air/solution interface, where the solution contains one of the redox mediators listed above [69]. To perform this experiment, the potential of the UME tip is set to a value to reduce a redox mediator such as $Ru(NH_3)_6^{3+}$, for example. The tip current is monitored as the tip is moved from air into the solution, and should resemble the approach curve shown in Figure 5. For a well-insulated tip, when the tip first enters the solution, the current rises sharply, passes

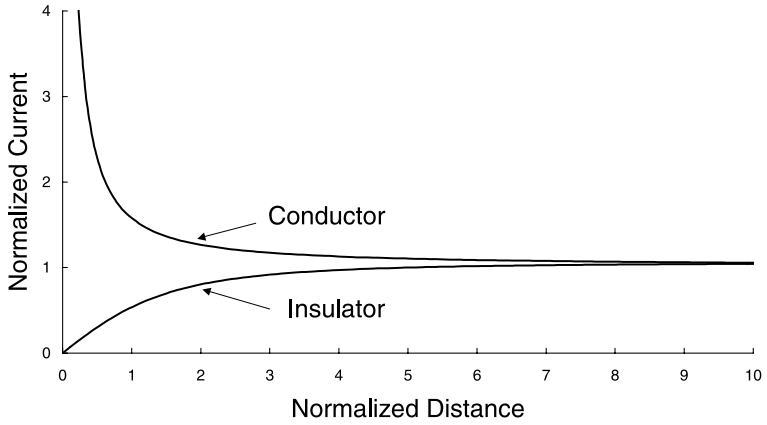

Fig. 4. Theoretical SECM approach curves for an inlaid disk UME ($RG \geq 10$) in solution over an infinite conducting or insulating substrate.

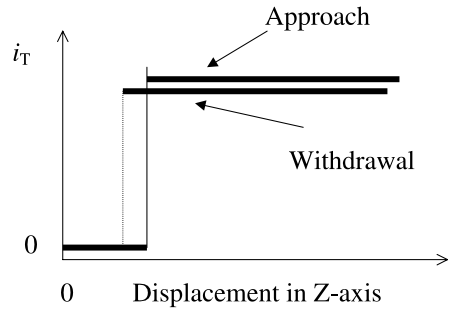

Fig. 5. Ideal electrochemical approach curves of a UME tip with good insulation to an air/solution interface. The solution would contain a reversible redox mediator such as $Ru(NH_3)_6^{3+}$.

through a brief transient, and then attains the steady-state current value $i_{T,\infty}$, and maintains this constant value as more of the tip is immersed into the solution. In the reverse scan where the UME tip is withdrawn from solution to air, a corresponding response is observed except that there is a gap in distance caused by the surface tension of the solution that allows a small amount of solution to be held on the tip as it crosses the air/solution interface.

10. A Look Ahead

The exploitation of UMEs, nanoelectrodes in particular, will continue as scanning probe techniques are further developed and carried out in concert with each other (e.g., SECM/AFM, SECM/OM, SECM/NSOM), as novel interfaces are probed (e.g., gas/liquid, monolayers), and as increasingly smaller environments (e.g., cells, pores, microscopic active electrode sites) are investigated. Thus, a push in UME fabrication will continue in the direction of sturdy and/or disposable nano- and Angstrom-sized UMEs. UME geometries likely to receive increased attention include recessed-disk UMEs [117 – 119] and carbon nanotube UMEs [120]. A continued desire to have more control over electrode geometry and increased reproducibility in the fabrication process will ensure the development of new microfabrication techniques in fabricating individual UMEs. New methods of UME insulation and characterization will also continue to be developed. New theory describing the behavior of UMEs smaller than 10 nm will need to keep pace with fabrication techniques and novel UME applications.

11. Acknowledgements

Support from the Georgia State University Research Initiative is acknowledged, as are the helpful comments of Allen Bard during the writing of this review.

12. References

[1] G. E. Loeb, R. A. Peck, J. Martyniuk, *J. Neurosci. Methods* **1995**, *63*,175.
[2] R. M. Wightman, *Anal. Chem.* **1981**, *53*, 1125A.
[3] *Ultramicroelectrodes* (Eds: M. Fleischman, S. Pons, D. R. Rolison, P. P. Schmidt), Datatech Systems, Morganton, NC **1987.**
[4] S. Pons, M. Fleischman, *Anal. Chem.* **1987**, *59*, 1391A.
[5] *Microelectrodes: Theory and Applications*, NATO ASI Series, Vol. 197 (Eds: M. I. Montenegro, M. A. Qukeiros, J. L. Daschbach), Kluwer, Dordrecht **1991.**
[6] J. Heinze, *Angew. Chem. Int. Ed. Engl.* **1993**, *32*, 1268.
[7] R. J. Forster, *Chem. Soc. Rev.* **1994**, 289.
[8] C. Amatore, in *Physical Electrochemistry* (Ed: I. Rubinstein), Marcel Dekker, New York, **1995**, ch. 4.
[9] C. G. Zoski, in *Modern Techniques in Electroanalysis* (Ed: P. Vanysek) Wiley-Interscience, New York, **1996**, ch. 6.
[10] R. M. Wightman, D. O. Wipf, in *Electroanalytical Chemistry*, Vol 15 (Ed: A. J. Bard), Marcel Dekker, New York **1989**, p. 267.
[11] K. T. Kawagoe, J. B. Zimmerman, R. M. Wightman, *J. Neurosci. Methods* **1993**, *48*, 225.
[12] A. C. Michael, R. M. Wightman, in *Laboratory Techniques in Electroanalytical Chemistry* (Eds: P. T. Kissinger, W. R. Heineman), Marcel Dekker, New York **1996**, p. 367.
[13] R. A. Clark, S. E. Zerby, A. G. Ewing, in *Electroanalytical Chemistry*, Vol 20 (Eds: A. J. Bard, I. Rubinstein), Marcel Dekker, New York **1989**, p. 227.
[14] K. Stulik, C. Amatore, K. Holub, V. Marecek, W. Kutner, *Pure Appl. Chem.* **2000**, *72*, 1483.
[15] A. L. Barker, M. Gonsalves, J. V. Macpherson, C. J. Slevin, P. R. Unwin, *Anal. Chim. Acta* **1999**, *385*, 223.
[16] C. J. Slevin, S. Ryley, D. J. Walton, P. R. Unwin, *Langmuir* **1998**, *14*, 5331.
[17] M. Koudelka-Hep, P. D. van der Wal, *Electrochim. Acta* **2000**, *45*, 2347.
[18] P. J. S. Smith, P. G. Haydon, A. Hengstenberg, S.-K. Jung, *Electrochim. Acta* **2001**, *47*, 283.
[19] A. J. Bard, L. R. Faulkner, *Electrochemical Methods: Fundamentals and Applications*, Wiley, Chichester **2001**, ch. 5.
[20] R. Morris, D. J. Franta, H. S. White, *J. Phys. Chem.* **1987**, *91*, 3559.
[21] J. D. Norton, H. S. White, S. W. Feldberg, *J. Phys. Chem.* **1990**, *94*, 6772.
[22] R. M. Penner, M. J. Heben, T. L. Longin, N. S. Lewis, *Science* **1990**, *250*, 1118.
[23] R. Feeney, S. P. Kounaves, *Electroanalysis* **2000,** *12*, 677.
[24] R-I. Stefan, J. F. van Staden, H. Y. Aboul-Enein, *Crit. Rev. in Anal. Chem.* **1999,** *29*, 133.
[25] G. Denault, G. Nagy, K. Toth, in *Scanning Electrochemical Microscopy* (Ed.: A. J. Bard, M. V. Mirkin) Marcel Dekker, New York **2001**, 445 – 519.
[26] B. R. Horrocks, G. Wittstock, in *Scanning Electrochemical Microscopy* (Eds.: A. J. Bard, M. V. Mirkin) Marcel Dekker, New York **2001**, 445 – 519.
[27] A. J. Bard, F-R. Fan, M. V. Mirkin, in *Electroanalytical Chemistry*, Vol 18 (Ed: A. J. Bard), Marcel Dekker, New York **1994**, p. 243.
[28] D. O. Wipf, in *Current Protocols: Methods in Materials Research* (Ed: Kaufman) Wiley, Chichester, **2001.**
[29] F. R. F. Fan, C. Demaille, in *Scanning Electrochemical Microscopy* (Eds: A. J. Bard, M. V. Mirkin), Marcel Dekker, New York **2001**, pp. 75 – 110.
[30] P. Tschuncky, J. Heinze, *Anal. Chem.* **1995**, *67*, 4020.

[31] *Scanning Electrochemical Microscopy*, (Eds: A. J. Bard, M. V. Mirkin), Marcel Dekker, New York **2001.**
[32] B. D. Pendley, H. D. Abruna, *Anal. Chem.* **1990**, *62*, 782.
[33] G. Fish, O. Bouevitch, S. Kokotov, K. Lieberman, D. Palanker, I. Turovets, A. Lewis, *Rev. Sci. Instrum.* **1995**, *66*, 3300.
[34] Y. H. Shao, M. V. Mirkin, G. Fish, S. Kokotov, D. Palanker, A. Lewis, *Anal. Chem.* **1997**, *69*, 1627.
[35] X. Zhang, B. Ogorevc, *Anal. Chem.* **1998**, *70*, 1646.
[36] B. B. Katemann, W. Schuhmann, *Electroanalysis* **2001**, *14*, 22.
[37] M. A. Dayton, J. C. Brown, K. J. Stutts, R. M. Wightman, *Anal. Chem.* **1980**, *52*, 946.
[38] R. S. Kelly, R. M. Wightman, *Anal. Chim. Acta*, **1986**, *187*, 79.
[39] R. Bravo, C. C. Hsuch, A. Jamarillo, A. Brajter-Toth, *Analyst* **1998**, *123*, 1625.
[40] K. A. El-Nour, A.Brajter-Toth, *Electroanalysis* **2000**, *12*, 805.
[41] D. K. Y. Wong, L. Y. F. Xu, *Anal. Chem.* **1995**, *67*, 4086.
[42] M. McNally, D. K. Y. Wong, *Anal. Chem.* **2001**, *73*, 4793.
[43] D. T. Miles, A. Knedlik, W. O. Wipf, *Anal. Chem.* **1997**, *69*, 1240.
[44] G. Zhao, D. M. Giolando, J. R. Kirchhoff, *J. Electroanal. Chem.* **1994**, *379*, 505.
[45] G. Zhao, D. M. Giolando, J. R. Kirchhoff, *Anal. Chem.* **1995**, *67*, 2592.
[46] J. P. Bozon, D. M. Giolando, J. R. Kirchhoff, *Electroanalysis* **2001**, *13*, 911.
[47] K. R. Wehmeyer, R. M. Wightman, *Anal. Chem.* **1985**, *57*, 1989.
[48] J. Golas, Z. Galus, J. Osteryoung, *Anal. Chem.* **1987**, *59*, 389.
[49] Z. Stojk, J. Osteryoung, *Anal. Chem.* **1989**, *61*, 1305.
[50] Y. Selzer, D. Mandler, *Anal. Chem.* **2000**, *72*, 2383.
[51] C. Demaille, M. Brust, M. Tsionsky, A. J. Bard, *Anal. Chem.* **1997**, *69*, 2323.
[52] M. Brust, D. Bethell, D. J. Schiffrin, C. Kiely, *Anal. Chem.* **1995**, *7*, 795.
[53] D. Bethell, M. Brust, D. J. Schiffrin, C. Kiely, *J. Electroanal. Chem.* **1996**, *409*, 137.
[54] D. R. MacFarlane, D. K. Y. Wong, *J. Electroanal. Chem.* **1985**, *185*, 197.
[55] A. M. Bond, M. Fleischmann, S. B. Khoo, S. Pons, J. Robinson, *Indian J. Technol.* **1986**, *24*, 492.
[56] A. Russell, K. Repka, T. Dibble, J. Ghoroghchian, J. J. Smith, M. Fleischmann, C. H. Pitt, S. Pons, *Anal. Chem.* **1986**, *58*, 2961.
[57] Y.-T. Kim, D. M. Scarnulis, A. G. Ewing, *Anal. Chem.* **1986**, *58*, 1782.
[58] R. A. Saraceno, A. G. Ewing, *Anal. Chem.***1988**, *60*, 2016.
[59] L. S. Kuhn, A. Weber, S. G. Weber, *Anal. Chem.* **1990**, *62*, 1631.
[60] C. B. Cohen, S. G. Weber, *Anal. Chem.* **1993**, *65*, 169.
[61] G. I. Pennarun, C. Boxall, D. O'Hare, *Analyst* **1996**, *121*, 1779.
[62] N. Casillas, P. James, W. H. Smyrl, *J. Electrochem. Soc.* **1995,** *142*, L16.
[63] P. James, N. Casillas, W. H. Smyrl, *J. Electrochem. Soc.* **1996,** *143*, 3853.
[64] G. Shi, L. F. Garfias-Mesias, W. H. Smyrl, *J. Electrochem. Soc.* **1998,** *145*, 2011.
[65] E. Betzig, J. K. Trautman, T. D. Harris, J. S. Weiner, R. L. Kostelak, *Science* **1991**, *251*, 1468.
[66] E. Betzig, A. Lewis, A. Harootunian, M. Isaacson, E. Kratschmer, *Biophysical J.* **1986**, *49*, 269.
[67] A. Lewis, K. Lieerman, *Anal. Chem.* **1991**, *63*, 625A.
[68] E. Betzig, J. K. Trautman, *Science* **1992**, *257*, 189.
[69] Y. Lee, A. J. Bard, *Anal. Chem.* **2001**, in press.
[70] Y. Lee, S. Amemiya, A. J. Bard, *Anal. Chem.* **2001**, *73*, 2261.
[71] H. Shiku, R. C. Dunn, *Anal. Chem.* **1999**, *71*, 23A.
[72] R. C. Dunn, *Chem. Rev.***1999**, *99*, 2891.
[73] M. A. Paesler, P. J. Moyer, *Near-Field Optics: Theory, Instrumentation, and Applications* **1996**, Wiley, New York.
[74] J. K. Trautman, J. J. Macklin, L. E. Brus, E. Betzig, *Nature* **1994**, *369*, 40.
[75] G. Zhao, D. M. Giolando, J. R. Kirchhoff, *Anal. Chem.* **1995**, *67*, 1491.
[76] P. Lilheroth, C. Johans, C. J. Slevin, B. M. Quinn, K.Kontturi, *Elecctrochem. Comm.* **2002**, *4*, 67.
[77] Y. H. Lee, G. T. Tsao, P. C. Wankant, *Ind. Eng. Chem. Fundam.* **1978**, *17*, 59.
[78] L. A. Nagahara, T. Thundat, S. M. Lindsay, *Rev. Sci. Instrum.* **1989**, *60*, 3128.
[79] R. M. Penner, M. J. Heben, N. S. Lewis, *Anal. Chem.* **1989**, *61*, 1630.
[80] M. V. Mirkin, F-R. F. Fan, A. J. Bard, *J. Electroanal. Chem.* **1992**, *328*, 47.
[81] F-R. F. Fan, M. V. Mirkin, A. J. Bard, *J. Phys. Chem.* **1994**, *98*, 1475.
[82] C. J. Slevin, N. J. Gray, J. V. Macpherson, M. A. Webb, P. R. Unwin, *Electrochem. Commun.* **1999**, *1*, 282.
[83] J. L. Conyers, H. S. White, *Anal. Chem.* **2000**, *72*, 4441.
[84] P. Sun, Z. Zhang, J. Guo, Y. Shao, *Anal. Chem.* **2001**, *73*, 5346.
[85] J. V. Macpherson, P. R. Unwin, *Anal. Chem.* **2000**, *72*, 276.
[86] T. Abe, K. Itaya, I. Uchida, *Chem. Lett.* **1988**, 399.
[87] A. A. Gewirth, D. H. Craston, A. J. Bard, *J. Electroanal. Chem.* **1989**, *261*, 477.
[88] C. M. Vitus, S. C. Chang, M. J. Weaver, *J. Phys. Chem.* **1991**, *95*, 7559.
[89] B. Zhang, E. Wang, *Electrochim. Acta* **1994**, *39*, 103.
[90] C. E. Bach, RlM. Nichols, H. Meyer, J. O. Besenhard, *Surf. Coatings Technol.* **1994**, *67*, 139.
[91] C. E. Bach, R. J. Nichols, W. Beckman, H. Meyer, A. Schulte, J. O. Besenhard, P. D. Jannakoudakis, *J. Electrochem. Soc.* **1993**, *140*, 1281.
[92] B. W. Mao, J. H. Ye, X. D. Zhuo, J. Q. Mu, Z. D. Fen, Z. W. Tian, *Ultramicroscopy* **1992**, *42 – 44*, 464.
[93] K. Potje-Kamloth, J. Janata, M. Josowicz, *Ber. Bunsenges. Phys. Chem.* **1993**, *93*, 1480.
[94] T. G. Strein, A. G. Ewing, *Anal. Chem.* **1992**, *64*, 1368.
[95] A. Schulte, R. H. Chow, *Anal. Chem.* **1996**, *68*, 3054.
[96] T. G. Strein, *J. Electroanal. Chem.* **1991**, *138*, 254C.
[97] C. Lee, C. J. Miller, A. J. Bard, *Anal. Chem.* **1991**, *63*, 78.
[98] C. Kranz, G. Friedbacher, B. Mizaikoff, A. Lugstein, J. Smoliner, E. Bertagnolli, *Anal. Chem.* **2001**, *73*, 2491.
[99] W-H. Huang, D-W. Pang, H. Tong, Z-L. Wang, J-K. Cheng, *Anal. Chem.* **2001**, *73*, 1048.
[100] S. Chen, A. Juccernak, *Electrochem. Commun.* **2002**, *4*, 80.
[101] G. Schurmann, P. F. Indermuhle, U. Staufer, N. F. de Rooij, *Surf. Interface Anal* **1999**, *27*, 299.
[102] P. Thiebaud, C. Beuret, N. F. de Rooig, M. Koudelka-Hep, *Sen. Actuators B* **2000**, *70*, 51.
[103] K. L. Saenger, G. Costrini, D. E. Kotecki, K. T. Kwietniak, P. C. Andricacos, *J. Echem. Soc.* **2001**, *148*, C758.
[104] D. C. Johnson, W. R. LaCourse, *Anal. Chem.* **1990**, *62*, 589A.
[105] D. S. Austin-Harrison, D. C. Johnson, *Electroanalysis*, **1989**, *1*, 189.
[106] D. S. Auston, J. A. Polta, T. Z. Polta, A. P.-C. Tang, T. D. Cabelka, D. C. Johnson, *J. Electroanal. Chem.* **1984**, *168*, 227.
[107] L. E. Welch, W. R. LaCourse, D. A. Mead, D. C. Johnson, *Anal. Chem.* **1989**, *61*, 555.

[108] T. G. Strein, A. G. Ewing, *Anal. Chem.*, **1993**, *65*, 1203.
[109] A. J. Bard, L. R. Faulkner, *Electrochemical Methods: Fundamentals and Applications,* 2nd ed., Wiley, New York **2001**, pp. 569–571, 654–656.
[110] K. Kinoshita, *Carbon-Electrochemical and Physiochemical Properties*, Wiley, New York **1987.**
[111] R. L. McCreery, in *Electroanalytical Chemistry*, Vol. 17 (ED. A. J. Bard), Marcel Dekker, New York, **1991**, 221.
[112] L. Otero, N. Vettorazzi, L. Sereno, *J. Electrochem. Society* **2001**, *148*, E413.
[113] J. Zhou, D. O. Wipf, *J. Electroanal. Chem.* **2001**, *499*, 121.
[114] W. Miao, Z. Ding, A. J. Bard, *J. Phys. Chem. B* **2002**, *106*, 1392.
[115] M. von Stackelberg, M. Pilgram, W. Toome, *Z. Elektrochem.* **1953**, *57*, 342.
[116] C. G. Zoski, M. V. Mirkin, *Anal. Chem.* **2002**, *72*, 1986.
[117] F-R. F. Fan, A. J. Bard, *Science* **1995**, *267*, 871.
[118] F-R. F. Fan, J. Kwak, A. J. Bard, *J. Am. Chem. Soc.* **1996**, *118*, 9669.
[119] A. J. Bard, F-R. F. Fan, *Acc. Chem. Res.* **1996**, *29*, 572.
[120] J. K. Campbell, L. Sun, R. M. Crooks, *J. Am. Chem. Soc.* **1999,** *121*, 3779.